applied sciences

MDPI

Article

Scoliosis Brace Finite Element Model and Preliminary Experimental Testing Using Electronic Speckle Pattern Interferometry

Slawomir Grycuk [1] and Piotr Mrozek [2,*]

[1] Faculty of Mechanical Engineering, Doctoral School of Bialystok University of Technology, Wiejska 45A, 15-351 Bialystok, Poland; s.grycuk@doktoranci.pb.edu.pl
[2] Institute of Biomedical Engineering, Faculty of Mechanical Engineering, Bialystok University of Technology, Wiejska 45C, 15-351 Bialystok, Poland
* Correspondence: p.mrozek@pb.edu.pl

Abstract: This article presents the results of numerical finite element method (FEM) simulations in the Ansys environment of a Boston orthopaedic brace. The geometric model was developed based on the results of digitisation performed by means of a three-dimensional (3D) optical scanner. A test stand for measurement of the brace's field of displacements, utilising a laser electronic speckle pattern interferometer (ESPI), was used to experimentally verify the FEM model. During experimental testing, special attention was given to applying the loads and boundary conditions used in the numerical simulations. As a result, the relative difference between the experimentally and numerically determined displacements in the central part of orthoses amounted to approximately 0.6%. The experimentally verified FEM model was used to determine the force flow lines characteristic of the brace, indicating the general working method of the brace's structure. The primary parts of the orthoses, carrying loads correcting the spine and the position of sites exerting little effort from the perspective of their participation in the orthoses' essential therapeutic application were identified. The results obtained allow for the proposal of methods for mechanical optimisation of the brace's design. The analysis conducted is universal in nature and can be adapted to other types of orthopaedic braces.

Keywords: FEM; ESPI; out-of-plane displacement; orthoses; principal stress trajectories; principal stress vector; force flow lines

Citation: Grycuk, S.; Mrozek, P. Scoliosis Brace Finite Element Model and Preliminary Experimental Testing Using Electronic Speckle Pattern Interferometry. *Appl. Sci.* **2022**, *12*, 3876. https://doi.org/10.3390/app12083876

Academic Editor: Zimi Sawacha

Received: 16 March 2022
Accepted: 8 April 2022
Published: 12 April 2022

1. Introduction

Scoliosis is a serious three-dimensional (3D) spinal deformity [1]. Scoliosis is treated with non-surgical methods such as the use of orthoses, for example, the Boston brace [2]. A brace is a customised thoracic orthosis. It is typically quite rigid and heavy. In practice, from the time of diagnosis until the body reaches physical adulthood, the patient has to wear a brace for more than 23 h a day to achieve treatment results [3]. The simplest corrective action of the orthoses involves the application of forces at the top of the curvature of the spine and at the support points at two places on the other end. This is the so-called three-point pressure system [4]. Advanced designs, for example, the Cheneau orthosis, are based on the use of a multiple three-point correction scheme in 3D space [5]. Improper methods of applying forces would result in ineffective therapy or, in the worst case, an increase in spinal curvature.

Currently, computerised methods are increasingly being used to design braces. Two main approaches can be distinguished. The first, which can be seen, for example, in the design of the CtrlBrace, uses computer-aided design (CAD) and computer-aided manufacturing (CAM) and involves taking measurements of the patient's torso without posture correction, followed by modelling of the corrective brace's geometry by means of a CAD/CAM operation, carried out by an experienced, professional orthotics designer [2,6–8]. The second approach, for example in the case of NewBrace [9], focuses on the use of torso geometry described by the finite element method (FEM) for design purposes. To this end, the results

of computed tomography (CT) or magnetic resonance (MR) medical imaging, and sometimes a 3D scan of the torso, are used, from which a body model is obtained, representing the actual structure of the musculoskeletal system [6,9–11]. The geometric image of the torso's FEM model, after correction by the computer-modelled spatial field of pressures, is used as the model of the brace's geometry. Due to the difficult issue of contact and the presence of complex anatomical structures in the human torso, in practice, it is not possible to faithfully represent FEM-determined fields of corrective pressures on the torso. In articles by Cobetto et al. [9] and Weiss and Kleban [12], the authors compare the effectiveness of braces designed using CAD/CAM computer methods combined with FEM. They emphasise that each of these methods has its pros and cons, and that combining them may bring about better efficacy of bracing. The efficacy of action of the designed braces can be practically verified, for example, through X-ray or CT imaging of the patient wearing the brace.

In research, experiments to determine the forces generated in orthosis components, such as the straps that tighten the orthosis, during corrective work, or the forces acting on the orthosis, are important in brace design research. For example, arrays with a large number of pressure sensors placed inside the orthosis are used [13–15]. Two research directions may be identified. In the first variant, testing is carried out involving the patients [13]. In the other variant, a standard force test stand with three-point loading of the orthoses is used [16].

It can be seen that the current progress in rigid orthoses is focused on a better comprehension of their correction functionalities [4], which are defined, inter alia, by the spatial force field required to act on the trunk, as well as, although less so, by the mechanical characteristics of the orthoses that are required to perform those functionalities. Examples of FEM applied to describe individual braces as an additional option accompanying FEM modelling of the torso can be found in the literature [17], but these brace designs are simplistic and fail to adequately replicate real brace geometry. Liao et al. [13] presented a more accurate model, but the results of FEM analysis pertained solely to the narrow problem of topological optimisation of the design, without a detailed analysis of the distribution of stresses and deformations in the orthoses structure.

Due to the nature of the structure, 3D modelling of the orthosis structure appears to be a challenging exercise. They are thin-walled, have cross-sectional openness and are subject to spatial force distribution. The relationship between the mechanical properties of the orthosis material and the pressures applied by the brace is debated in the literature [1]. Rigid orthoses are better at exerting corrective forces, while flexible ones tend to be more comfortable to use. There is an extensive literature on the subject of determining the distributions of corrective forces [3,7,8], but there is little information on the subject of the orthosis design's mechanical properties, which are indispensable for effecting these forces [11,14]. Analysis of the literature indicates that the proper directions and amounts of the correction forces in an orthosis are a determining factor in its effectiveness. Therefore, the mechanical requirements that the orthosis must meet to ensure its ability to realise the required pressure fields appear to be equally important. It seems that an analysis of principal stress vectors and determination of force flow lines based on them can provide more information about the orthosis. This is one of the many directions used in issues concerning the optimisation of mechanical structures, but the literature lacks detailed information on the work of the brace itself.

The influence of the brace structure on its functional properties, such as: weight, the level of the patient's thermal comfort, the level of gas exchange between the torso and the environment, and compliance to therapy, is not only an application issue, but also has a significant scientific importance. The problem of reducing the amount of brace material while increasing its functional properties and maintaining the unchanged corrective function is a big challenge. It seems that this task can only be solved with the use of advanced methods of analysis of the mechanical structure of the orthosis. The results of this analysis and the applied design improvements can obviously affect all medical aspects of the use of the

orthosis and, most importantly, the assessment of the orthosis from the patient's point of view. It seems that the presented methods of designing braces have a varying impact on increasing their functional parameters, important from the patient's perspective. This article proposes a brace design analysis, which includes the possibility of preserving the material in places where it is necessary to ensure the unchanged corrective function of the orthosis. It seems that this type of analysis procedure should lead to the proposal of the lightest and the most functional brace structure for the patient. One may pose the hypothesis that the development of a reliable numerical model of a real orthosis, whose effectiveness has been proven in practice, is the best starting place to analyse the mechanical properties of orthosis designs. The results of in-depth modelling of such designs are rarely found in the literature. The goal of the numerical simulations and experimental tests presented in this article is to develop a reliable, experimentally verified FEM model of an exemplary orthosis. An in-depth model analysis will be used as the foundation for defining the performance scheme of the orthosis design, allowing potential opportunities for design optimisation to be identified.

2. Materials and Methods

2.1. Boston Brace as a Research Subject

The Boston brace system's purpose is to enable non-surgical scoliosis treatment by attempting to prevent the progression of scoliosis in growing patients [18]. Generally, the system is effective when applied to arcs with an apex among T-6 and L-3. A Boston brace is usually ineffective for curves with apexes outside of this range [16]. In this regard, a Boston brace cannot be rigid in its top section and must only rest on the patient's armpits to protect the orthoses from shifting.

For this study, a Boston brace for the treatment of the left lumbar curve was chosen. A 4 mm thick sheet of polypropylene was thermally moulded into an orthosis. Polyurethane foam was used to line the inside of the orthoses. An example of a Boston brace and a diagram of the scoliosis described above are presented in Figure 1. In comparison to other types of orthoses, such as the Cheneau brace, which has a spatial system of several corrective forces, the Boston brace has a three-point system of corrective forces [19]. Forces F_1 and F_3 act on the spine by exerting pressure on the ribs, while force F_2 acts on the pelvis. Vector F_3 is the corrective force, and vectors F_1 and F_2 make up the counteracting force. The application of a relatively simple system of forces makes it possible to simplify the model and thus create a more plausible numerical model.

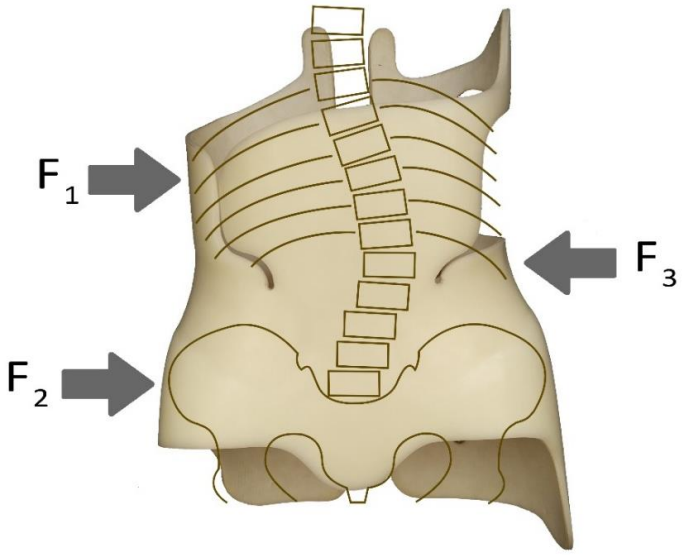

Figure 1. Boston brace—diagram of the left lumbar curve with a simplified correction scheme (view from front). Forces exerted by the brace: F_1 and F_3—forces acting on the thoracic cage, F_2—force applied to the pelvis.

In the conducted research, it was proposed to modify the brace structure in such a way that it does not change the distribution of the corrective forces of the orthosis after optimizing its structure. Thus, the assumed pressure distribution on the trunk should remain unchanged. Point loads were assumed in the model. In a real case, the corrective forces of the orthosis are distributed over a certain body surface while keeping the pressure values within the allowable range. The issue of modelling the brace pressures on the torso is complex and has been devoted a lot of space in the literature, therefore it was not the subject of experimental research in this work.

2.2. Test Stand for Experimental Verification of FEM Results

A schematic drawing of the ESPI interferometer system is shown in Figure 2. The DPSS laser (1) beam is split by a plate beam splitter (2) into two coherent beams. The transmitted beam is diverged by diverging lens (3) and, after passing through polarizers (4), illuminates reference surface of diffuser made of ground glass (5) and passes through cube beam combiner (6). The beam split by beam splitter (2) is reflected by mirrors (7 and 8) and diverged by diverging lens (9). The diverged beam illuminates the object surface (10). Speckle patterns are generated by light-diffusive surfaces. After passing through cube beam combiner (6) and digital camera (11), the speckle patterns meet and interfere with each other on the image plane of the CMOS sensor. The resulting image is displayed on a computer monitor and transferred to the hard disc of the computer (12). As a result of subtraction of the current speckle image from the initial speckle image, a stationary correlation fringe pattern is obtained for a static deformation of surface. The ESPI interferometer used for the measurements under discussion was developed as part of research work described by Mrozek [20].

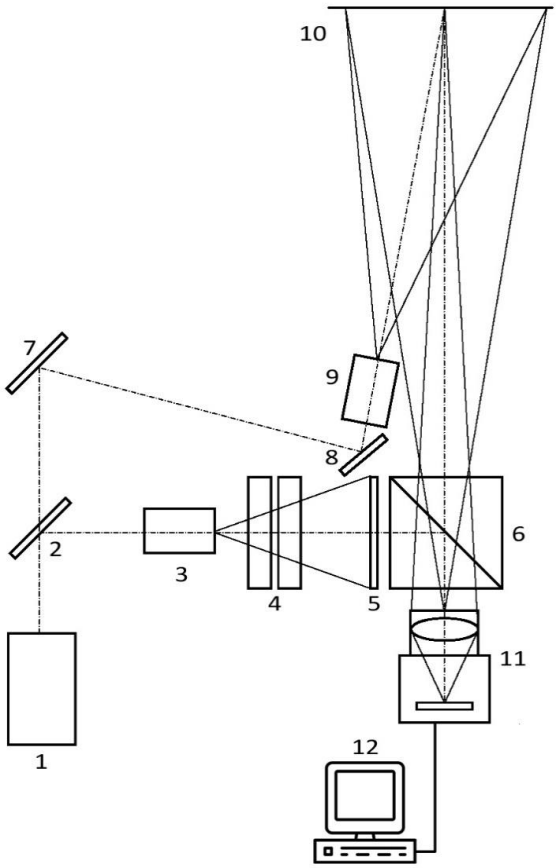

Figure 2. Schematic drawing of the ESPI interferometer: 1—laser, 2—plate beam splitter, 3 and 9—diverging lenses (100× microscope objective lens), 4—polarizers, 5—diffuser made of ground glass with a reference surface, 6—beam combiner, 7 and 8—mirrors, 10—object surface, 11—digital camera (CMOS), 12—computer.

A test stand for the measurement of orthopaedic braces was built and is presented in Figure 3. The stand consists of: optical bench (3), instrument for brace fastening (7) along with a pressure sensor (8), additional load application system (9) in the form of a tension member running over a rotary pulley with a 10 g weight, DPSS laser (1) emitting a beam with power of 50 mW and wavelength λ = 532 nm, optical set (2), digital camera (4), beam combiner (5) and computer with software (10). Together, components (1), (2), (4) and (5) form the electronic speckle pattern interferometer (ESPI). The divergence imposed on the brace to cover the whole object area (6) is 11.4°. The brace fastening instrument (7) allows for the application of preliminary load, stabilising the brace from the interior side of the brace, measured by the pressure sensor (8). Preliminary force A (Figure 5b) is applied by a support positioned inside the brace, as a result of the tensioning of the straps of the orthosis. The values of the brace displacements caused by this initial force exceed the measuring range of the interferometer and are not measured. Next, an additional force *D* of 0.1 N (Figure 5b), causing brace displacements within the measuring range of the interferometer, is applied close to the place of application of the preliminary force and implemented using system (9) consisting of a tension member, a 10 g weight and a pulley. Displacements of the brace as a result of loading with the additional force are registered and processed by the computer with software (10) [21]. The test stand is characterised by the simplification of the number and directions of the forces acting on the brace for the purpose of reflecting actual boundary conditions in the numerical model as accurately as possible. Through the application of the ESPI interferometer, information on the distribution of displacement fields Δz is determined for every point in the field of view of the interferometer's camera (Equation (1))

$$\Delta z = n \times \frac{\lambda}{2} \tag{1}$$

where: Δz—displacement value in nm, n—order of correlation fringe, λ—wavelength of emitted light (in this case 532 nm).

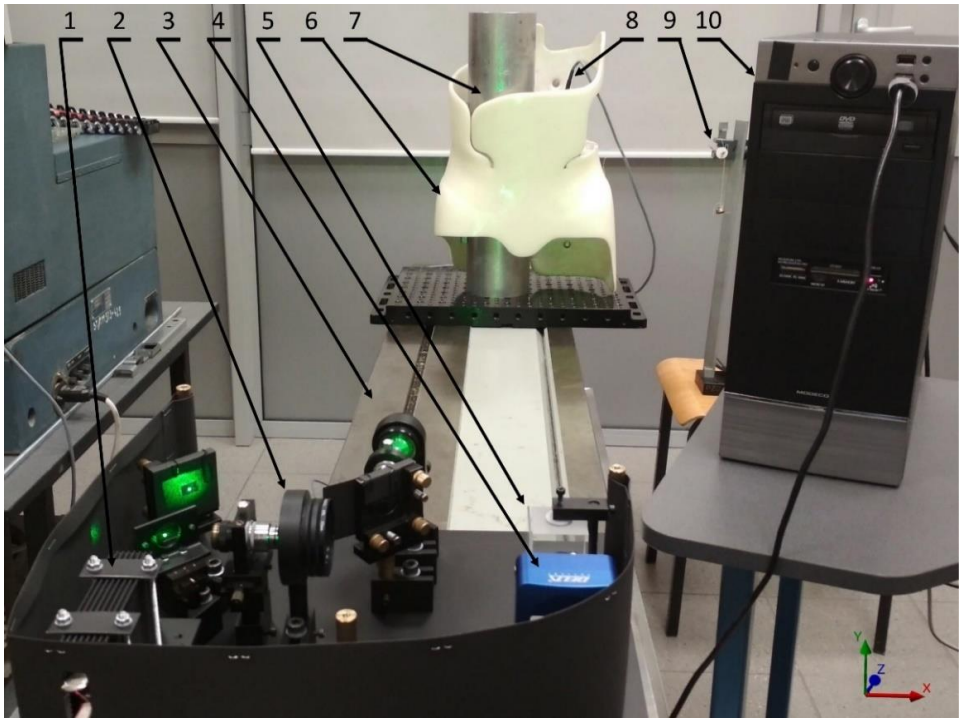

Figure 3. Brace test stand: 1—laser, 2—optical elements/optical set (beam splitter, lenses, polarisers), 3—bench, 4—digital camera (CMOS), 5—beam combiner with matte element, 6—tested object, 7—buckle for fastening and tightening of the brace, 8—pressure sensor, 9—system for application of additional load, 10—computer with software.

Using straps, the brace was tightened with a force of 36.25 N, which was measured by pressure sensor 8, the head of which was located at point *A* (Figure 5b) on the inside of the brace. Gravity also works on the orthosis that has been immobilised in this manner. After stabilisation of the brace, a force of 0.1 N was added at the site corresponding to point *D* in the numerical simulations (Figure 5b). The increase in displacements after the application of the additional force made up the result of the tests. The obtained results of the experimental measurements constitute the basis for verification of the correctness of the numerical simulations [22].

2.3. Geometric Model of Brace

Based on the existing orthosis shown in Figure 1, a 3-dimensional (3D) computer model of the orthosis was generated using reverse engineering techniques—3D scanning. As shown in Figure 4a, the braces were subjected to processes to prepare them for proper scanning [23]. The brace was stiffened for 3D measurement by adjusting the belt at the level of the drawstring straps (1). The surface of the orthosis was covered with matting material (2), and reference points (3) were pasted on to allow subsequent 3D scans to be spatially correlated. An optical scanner, the Atos Core 200 (GOM—a ZEISS company, Brunswick, Germany), was used to create the point cloud. After preliminary, rough processing, an STL triangle mesh represented as a binary mapping of 3,547,641 elements was obtained from the point cloud. For this purpose, 35 exposures were applied, using 28 markers. The fastening buckles were removed from the model, artefacts were repaired, and losses were filled in using Geomagic Wrap 2017 point cloud processing computer software (3D Systems, Rock Hill, SC, USA). A representation of the outer surface of the brace was created on such a modified mesh. The next step was to create, on the basis of this surface, a 4 mm thick shell that corresponds to the brace's structure as defined by NURBS splines. Through such processing of the point cloud, a model was created to represent the actual orthoses (Figure 4b). In addition, at the level of the apex of the spine curvature, an interior pad and a soft material corrective ring were modelled. The 3D model for the brace was created and then exported to the Ansys 2021 R2 (21.2) for finite element (FE) numerical calculations.

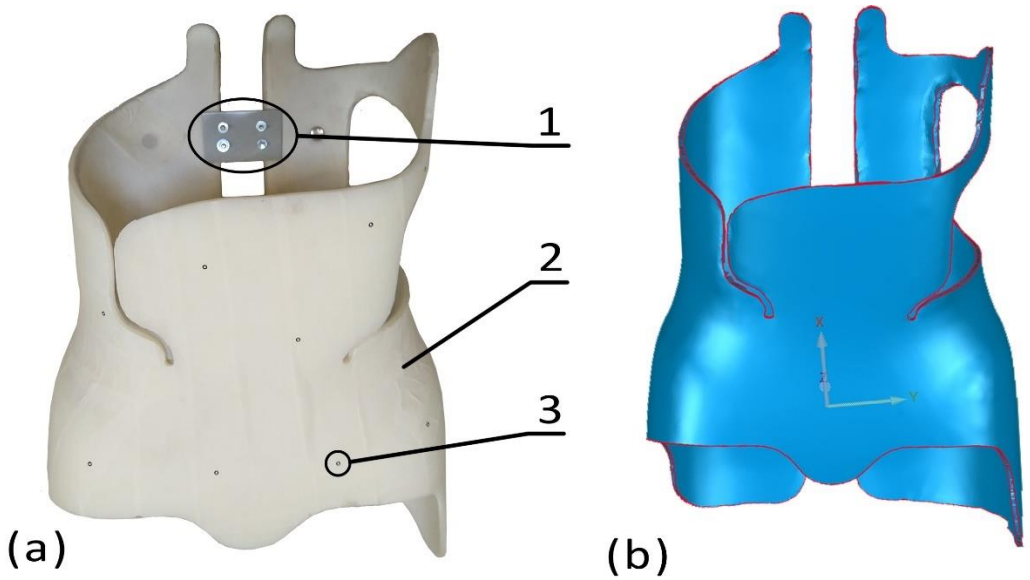

Figure 4. Reverse engineering as the process of creating a 3D model of an orthopaedic brace from the actual facility: (**a**) orthosis ready for scanning: 1—fixing brace stiffener, 2—matted outer layer of the orthoses, 3—reference markers, (**b**) CAD computer model of the orthosis.

2.4. FEM Model

The geometric conditions of the applied forces are, as far as possible, the same in experimental studies as in numerical analyses. Polypropylene was selected as the material of the exterior body (E = 1000 MPa, v = 0.2) [13,14]. The inner layer was modelled with soft foam (E = 100 MPa, v = 0.45) [14]. The 10-node tetrahedral element (SOLID187) was used to generate the FEM model. A relatively fine tetrahedral FE mesh (Figure 5a) was generated to demonstrate in detail the values and the distribution of directions of the principal stress vectors in each element separately. The tetrahedral shapes appear fairly regular, in spite of the complicated geometry of the orthoses. The mesh was also made more dense at critical locations with more complicated geometries to increase the accuracy of the calculation of the stresses arising during orthosis loading at these locations.

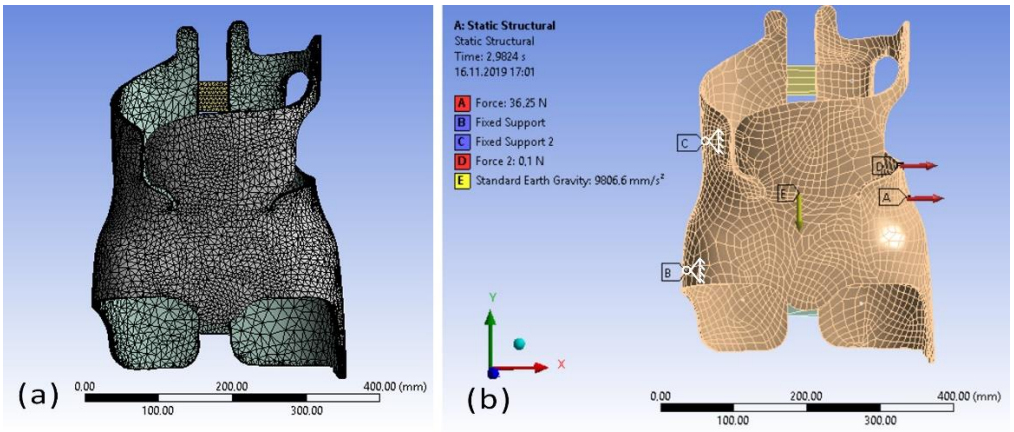

Figure 5. Numerical orthosis model: (**a**) tetrahedral FE mesh generated, (**b**) boundary conditions applied to the geometric model that has been imported; mathematical description (NURBS): *A*—pre-loading force corresponding to the action of the torso on the brace, *B* and *C*—fixed supports, *D*—additional force added after pre-loading of the orthosis, *E*—gravitational force.

Discretisation was carried out until further densification of the mesh of nodes did not change the resulting von Mises stress by over 3% [23]. Once concentration of the mesh was achieved, 199,187 nodes and 104,742 FE were obtained with a maximum edge dimension of 8.0 mm (Figure 5a). A relatively fine mesh of tetrahedral finite elements (Figure 4a) was generated in order to show in detail the distribution of directions and values of the principal stress vectors, shown after solving the problem in each element separately. The shapes of the tetrahedrons appear quite regular, despite the complex geometry of the brace.

After generation of the FE mesh and definition of the brace model's parameters, the boundary conditions that were applied in the experimental tests conducted as part of this research were introduced (Figure 5b). The three-point system of forces was implemented through the application of supports *B* and *C* and pre-loading force *A* (Figure 5b). Two immobile supports were set, defined as small surfaces *B* and *C*, immobilised in space. Preliminary loading of the brace was implemented as the application of load *A*, with a value of 36.25 N. The load of force A fits within the range of actual forces found in orthoses [24]. The application of the preliminary load was indispensable for stabilising the brace's position on the experimental test stand, which is described in Test stand for experimental verification of FEM results section. The orthosis immobilised in this way is also affected by the gravitational force *E*. To best represent the real conditions of the experiment, the gravitational force is included, although it does not appear to play much of a role. The displacement field has been calculated with the loads and supports thus defined. After performing the first step of the calculation as previously described, an extra force *D* of 0.1 N, corresponding to the experimental conditions, was added to the brace in the direction of the applied force *A*. The application of a secondary force, low in value, corresponded to the conditions of the experiment, based on determining the field of small displacements for the brace, measured by an interferometer with a narrow measuring

range. As shown later in the paper, the orthosis's material operates in a linear range for typically applied loads acting on the orthoses. Thus test results of small displacements at low loads can be related linearly to findings corresponding to higher operating brace loads. The final simulation result was obtained by calculating the displacement difference prior to and after the introduction of force *D*. Due to the fact that the interferometer measures displacement on the axis lengthwise along the camera lens, the results of the displacement calculations are presented along this direction. As a result, the displacements distribution on the *Z* axis was received, which was verified with the measurements performed on the experimental test stand.

3. Results

3.1. Model Verification Tests

The distribution of the brace's displacements, obtained by means of FEM numerical analysis, is presented in Figure 6a, and the distribution measured using ESPI is shown in Figure 6b. The displacement values in the experimental tests were determined from Equation (1), using the distribution of correlation fringes with orders of interference from 0 to 6 (Figure 6b). The maximum displacement on the Z axis in the numerical simulations amounted to 1.606 µm, and in measurements on the test stand to 1.596 µm. The colour of the presented correlation fringes is arbitrary due to the presentation of the experimental results being the effect of mathematical operations on the pixel brightness levels. The original interferogram bitmaps using the interferometer described in this article are in green (532 nm). The colour has been changed to red for high-contrast correlation fringes presentation.

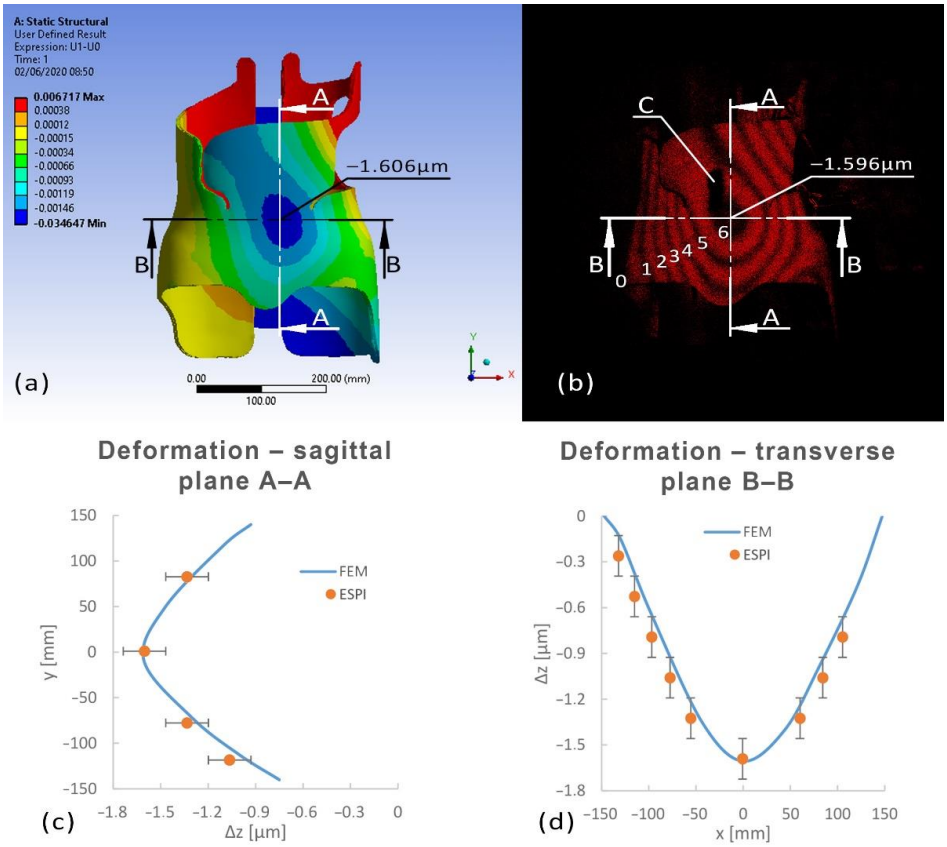

Figure 6. Comparison of displacement distribution results in the Z direction: (**a**) displacement distribution obtained from FEM numerical analysis, (**b**) displacement distribution obtained from ESPI measurements: numbers $n = 0, 1, \ldots, 6$, associated with the value of displacement according to Equation (1), indicate correlation fringes of successive orders of interference (C—artifact resulting from excessively intensive laser beam reflex), (**c**) deformation graph in the sagittal plane A–A, and (**d**) deformation graph in the transverse plane B–B.

3.2. Tests Using Verified Numerical Model

Using the numerical model, verified according to the method described above, tests were conducted under a load of the same order as used in other FEM studies [24], amounting to 30 N, applied at point A and consistent with the physiological loading. The distribution of von Mises stress was obtained, as illustrated in Figure 7. As well as sites with a relatively small area, at which the supports and force of loading were applied, the stresses in the majority of the orthosis were below 4.4 MPa (Figure 7) and fit in the linear region of the stress–strain curve of polypropylene [25], confirming the assumptions made earlier regarding the orthosis model.

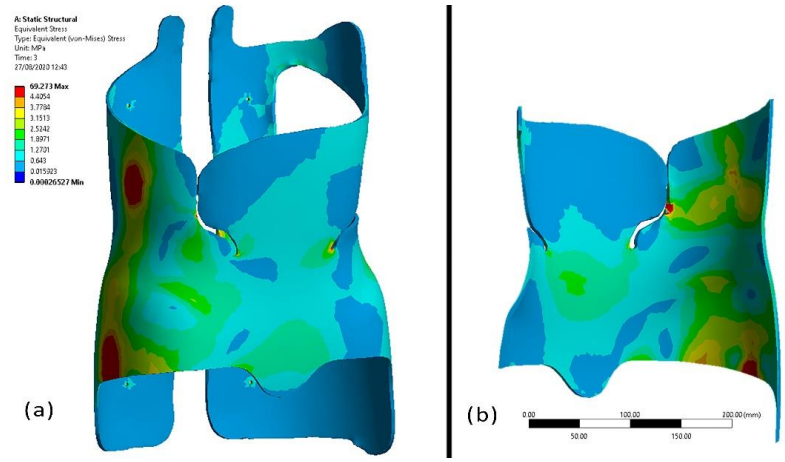

Figure 7. View of orthosis with values of von Mises stress: (**a**) left side—front from exterior, (**b**) right side—front from interior.

It can be seen from Figure 7 that it is hard to identify the working scheme of the orthosis. To more clearly present the method by which the orthosis's mechanical structure transmits loads, Figure 8 presents views of the front part of the brace that are shown to illustrate the principal stress vectors on the inside and outside of the front face of the orthosis.

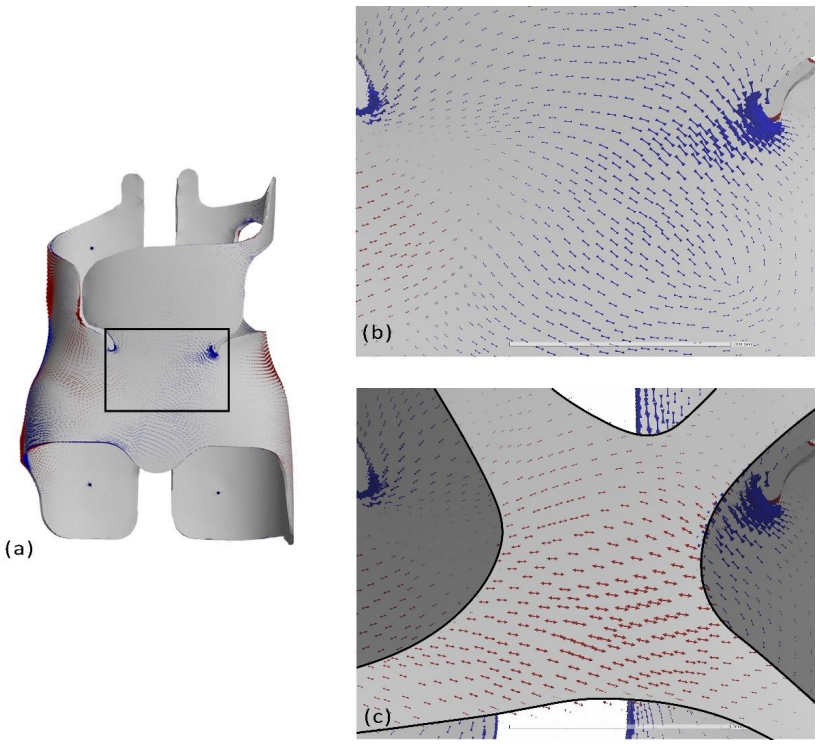

Figure 8. The principal stress distribution σ_1 (red) together with stress σ_3 (blue) in the region of the

orthosis's front part indicated in the illustration: (**a**) front part of the brace, (**b**) distribution of stresses on the outer face of selected region, (**c**) distribution of stresses in the cross-section of the front part of the brace; the inner wall layer is seen when "removing" some of the material of the outer wall.

Figure 9 shows the vectors of principal stresses solely for tensile stresses σ_1. In this illustration, the maximum principal stress trajectories σ_1 are plotted. Lines were laid parallel to the stress vector directions, starting and ending at the points of application of the applied external forces. The trajectories formed splines with mild changes in direction, tangent to σ_1 vectors.

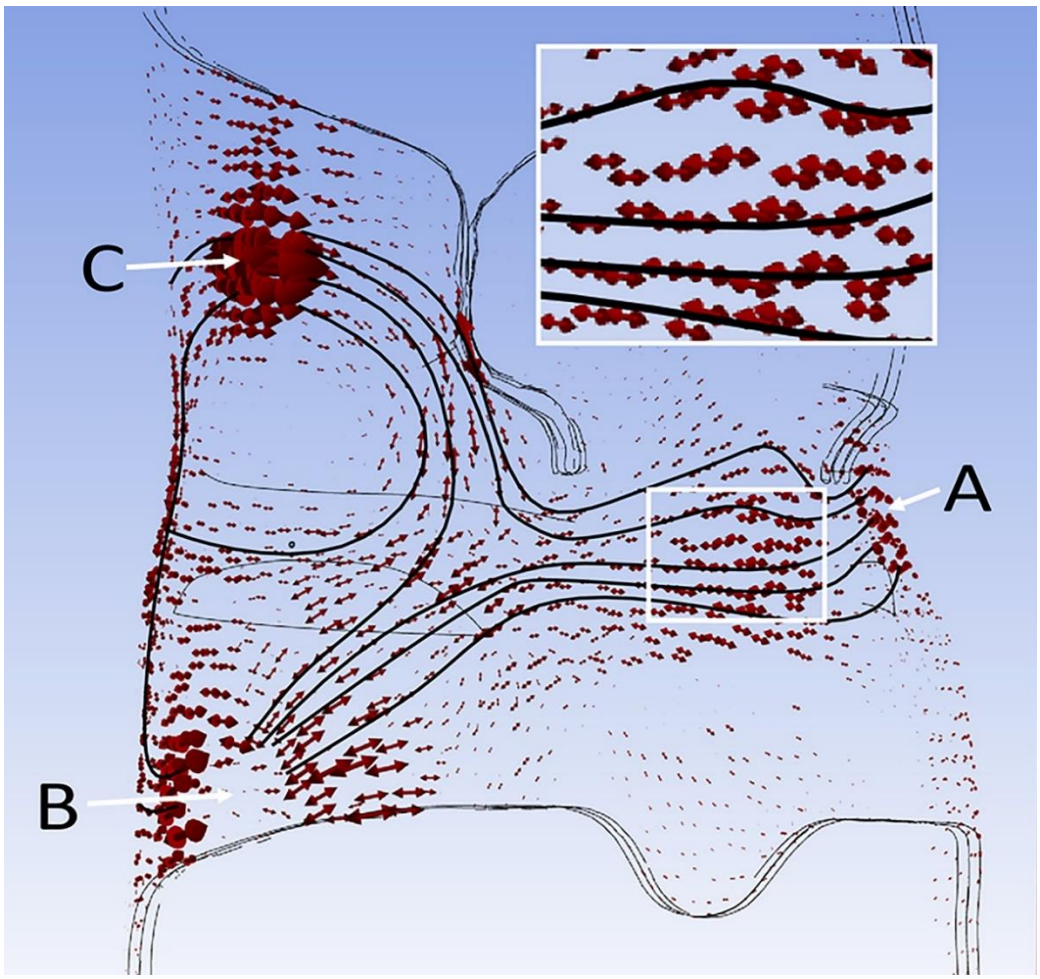

Figure 9. Principal tensile stress vector distribution with plotted trajectories of principal stress. Places where forces are applied: *A* and *C*—forces acting on the thoracic cage, *B*—force applied to the pelvis.

4. Discussion

A series of tests were carried out to differentiate the values of the applied external load in the three-point system of forces, without changing their points of application. The results of measurements of the displacement distribution were of a similar nature; therefore, the article presents a representative example of a three-point load case. This case of force distribution corresponds to a given variant of scoliosis. In the event of using a brace by the patient, the values of the forces exerted by the orthosis on the torso undergo certain changes, but the general nature of their distribution does not change because the patient's variant of scoliosis does not change. As a result, the nature of the distribution of strains and stresses in the brace does not change significantly. In the case of the three-point pressure principle, the results of the application of forces are unambiguous and immediate, which is confirmed by studies using ESPI and FEM.

The results of the model verification tests, presented in Figure 6, indicate the clear similarity between the distribution of displacement contour lines in the FEM image and the pattern of ESPI correlation fringes. A quantitative comparison of the obtained results of the numerical simulations with the experimental results shows that the relative difference in displacements in the central part of the brace's front wall, determined according to both methods, is small and amounts to approximately 0.6%. Despite the fact that only out-of-plane displacements of the brace were measured, their good compliance with the results of FEM calculations on the entire front surface, covering almost half of the brace, allows the conclusion that this method of model verification is sufficient. By using the linear-elastic relations, it allows one to conclude on the values of strains and stresses related to the displacement field. In uniaxial tension (compression), Hooke's law has the form (Equation (2))

$$\sigma = E\varepsilon \tag{2}$$

where: σ—normal stress, ε—strain, E—Young's modulus. It can therefore be accepted that the proposed method of describing the orthosis geometry, the applied values of the mechanical parameters of the materials used for modelling and, above all, the density of the mesh and type of finite elements used for FEM description, allow the development of a model with high correspondence between its mechanical characteristics and the characteristics of the actual object. As a result, it appears that using the FEM model for additional testing, using different variants and values of loading in distributions similar to those seen in real life, could provide a foundation to draw conclusions about the work of a real life brace.

Taking an approach in the direction defined in this way, a conventional analysis method of the FEM modelling results output was used, consisting of the calculation of the von Mises stress distribution at loads equal in order to the magnitude of the common correction loads, imposed in accordance with an elementary "three-point system". Figure 7 shows that the chosen thickness of the polypropylene shell provides the orthosis with the required strength parameters. Von Mises Equivalent stress is determined on the basis of strength hypotheses. Equivalent stress represents the action of all the component stresses in a loaded body and its value must be less than or equal to the critical stress depending on material yield strength and the assumed factor of safety. The von Mises stress values for this material are significantly below the allowable stress (F_α) values. Apart from the force application and support locations, the stress values in other parts of the orthosis were less than 4.4 MPa, consistent with the linear stress–strain curve characteristics of polypropylene [25]. It is possible to identify the areas of the orthosis that are most vulnerable to mechanical damage and those that do almost no work. Even if a similar "three-point system" was used, it might be hard to generalise the obtained results to orthosis cases with different applied load values and geometric parameters due to the quite irregular stress distribution in the orthosis body (Figure 7). As can be seen from von Mises stress calculations, the most stressed areas are the force application areas. In the study, very small force application areas were assumed in order to reduce the discrepancy between the experimental boundary conditions and the numerical model. In reality, the force application areas are larger and thus the stresses are much lower near force application areas. Nevertheless, the distribution of von Mises stresses, as shown in Figure 6 in areas other than the applied forces, obtain values significantly lower than the allowable stresses, indicating that the shell can be optimized. The principal stress distributions, which are shown in Figure 8 for different sections of the structure, seem to give more information in the general context of the performance of the orthoses. The outer surface of the front wall of the orthosis is in compression, while the inner face of the same wall is in tension. The values of absolute stresses on the interior side are approximately two times higher than those on the exterior layer. The rest of the shell of the brace works in a similar way. The characteristic stress distribution, characterised by a significant value of tensile stresses on the inside of the orthosis shell, is due to the superposition of stresses from two independently operating types of loads. The bracing shell is subjected to combined tension and bending states, as can be seen by comparing the signs and values of the stresses acting (Figure 10). This

observation is crucial to the proposal of the bracing optimisation method described later in this article, as it makes it possible to determine which site of the bracing wall is going to be subjected to the greatest tensile stress.

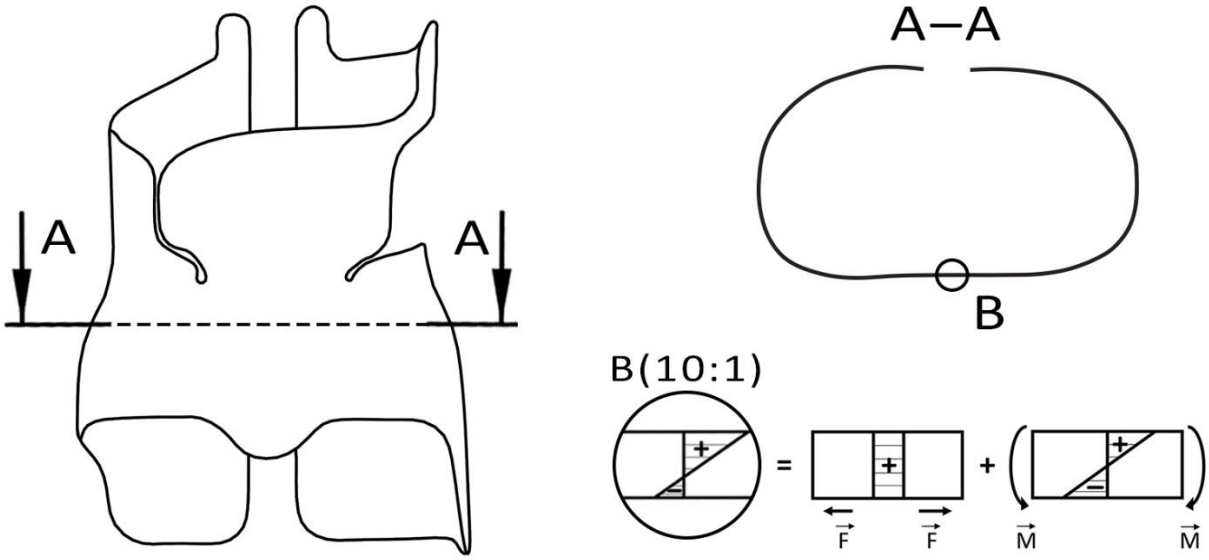

Figure 10. Stress distribution in section A–A of the front bracing wall (the upper side of diagram B corresponds to the inner side of the orthosis surface): superposition of stresses due to bending acting on moment *M* and force *F*.

Clear regularities shaping the obtained image of the lines can be seen from the determined vector fields of principal stresses and drawn maximum principal stresses σ_1 trajectories in the regions in which these stresses take relatively large values (Figure 9). The trajectories of the principal stresses follow a characteristic pattern, connecting the correction load locations along paths of a relatively small sum of lengths. This image depicts the "force flow lines" concept that is currently being intensively developed in the theory of optimal design [26]. It is based on the insight that, in principle, the "flow" of forces across a mechanical structure among external load application points is strongest near the topographic lines connecting these locations in space, taking into account the imposed limits of the geometry of the structure. Although trajectories of principal stress are one way to practically apply the idea of "force flow lines", the literature offers alternative rival proposals [27]. On the basis of this idea, the orthosis may be characterised as a space-based mechanical system that transmits loads along comparatively brief trajectories between locations where correction loads are applied. It seems that analysis of principal stress vectors can provide more information about the orthosis. Principal stresses describe the stress state represented by normal stresses only, with zero tangential stresses. They are a useful way of presenting force flow lines. The force flow line is a concept used to visualize the path of an applied load through a load bearing member. This is one of many methods used in issues of the optimisation of mechanical structures, which are intensively developed, but the literature lacks detailed information on the work of the brace itself. The analysis in the proposed paper deals with one particular force application scheme. The lines of force flow will change due to the type of loading scheme, but will be almost identical when changing only the values of forces. In this way, based on the space trajectories distribution presented in Figure 9, it is possible to determine the orthotic area responsible for performing the orthosis' correction function. Other regions perform a supportive role, for example, stabilising the orthosis against the body. In Figure 11a, areas of the orthosis structure that require less effort and have a supporting role are shown in the dark colour, while areas of the brace structure that require less effort and have a supporting role are shown in the light colour. The location of the correction region will be similar to that specified in the optimisation routine [13].

Nevertheless, in comparison with the approach of minimising the elastic energy in the method of topological optimisation, it appears the method presented above for analysing the performance of a structure is more comprehensible in the context of stress distribution analysis. There are no studies in the literature to date that have analysed principal stress for orthoses. On the basis of the numerical model analysis results shown previously, it is possible to propose methods for practical use. Based on the research findings, the weight of the orthosis can be reduced with no significant change in the mechanical performance of the orthosis, especially the orthosis stiffness in regions bearing correction loading. A simple solution may be to make the orthosis from thinner material by using an additional stiffener at the dark-coloured region in Figure 11a, which carries the corrective loads. The orthosis can be more rigid in this region by incorporating thin layers of composite with carbon or glass fibre reinforcement, orientated alongside the principal stress trajectory illustrated in Figure 11b. A comparison of Figures 7–9 clearly shows that the most effective overlap would be on the inner face at the front of the orthosis, as the inner face is subjected to a much higher loading in this region than the outer face. In the vicinity of the correction force points, the situation is reversed: the outer face bears considerably more load than the inner face, so overlays should be applied on the exterior, as shown in Figure 11c. In a similar way, locations for the overlays to be applied to other regions bearing correctional loads can be determined.

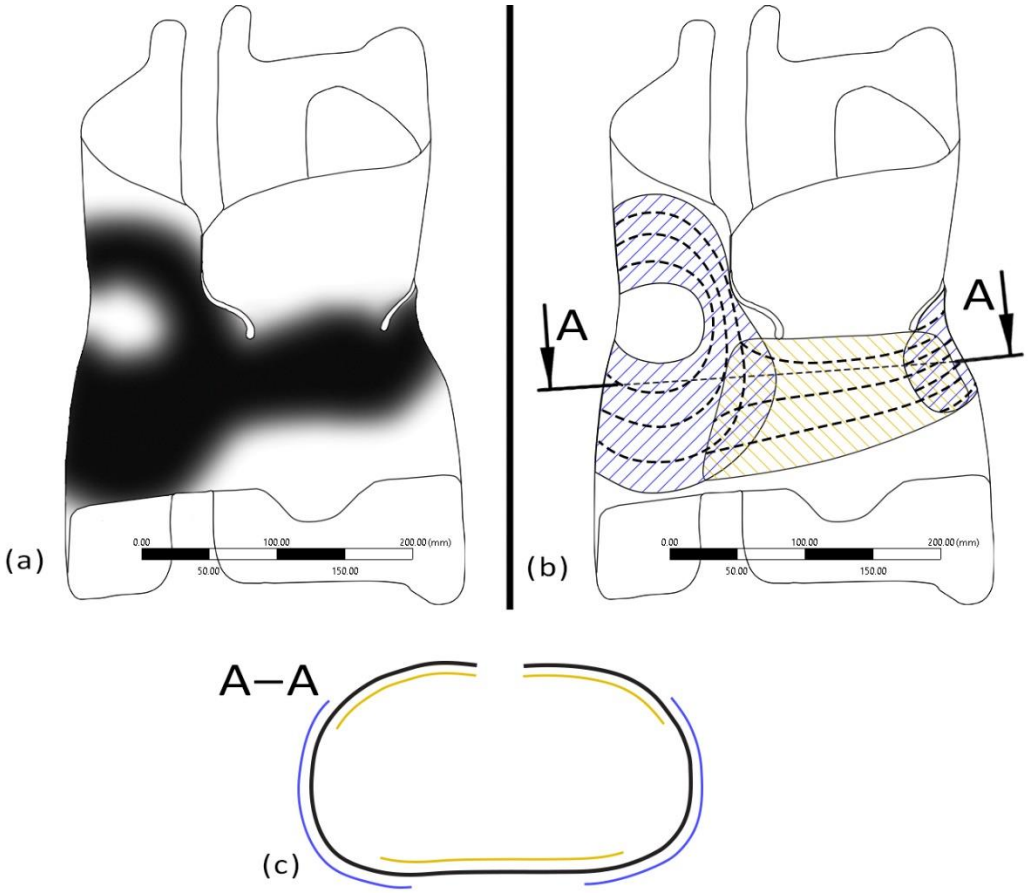

Figure 11. Boston brace: (**a**) area of the brace's structure exerting the greatest effort, performing a corrective role (dark colour), and the remaining area, playing an auxiliary role (light colour), (**b**) stiffening by integrating its surface with thin composite layers made of polypropylene reinforced with glass or carbon fibres that are arranged by the principal stress trajectories, (**c**) a cross-section showing the brace overlay positions; dashed lines—orientation of reinforcement fibres.

It can be seen from the above discussion that, for a three-point force system, it is fairly easy to predict the trajectory of the force flow line in the orthosis, which serves as the foundation for determining the regions that need strengthening. At its most basic,

the orthosis corrects the curvature using the principle of three-point compression, which consists of fixing below, above and on top of the curvature [28]. Selected experimental configurations mimic the physiological load as closely as possible. In difficult cases, the experimental stand and the numerical modelling need to consider the corresponding more complicated arrangements. However, it appears that the procedure described can be used to optimise orthosis design in these more complex cases as well. However, further numerical calculations are needed to verify that hypothesis. The other way to use the findings of the study in practise would be to remove material, for example, through drilling holes in regions that are irrelevant to the correction performance of the orthosis (the light-coloured area in Figure 11a).

The present trend in orthoses testing is to find a material that can be used as a replacement for polypropylene and can be printed using the FDM method [29]. The obtained results are an excellent contribution to this trend because they can form the basis for the development of a method for the realisation of a printed 3D design model supported on an openwork geometry that corresponds to the distribution of the trajectory of principal stresses, at the same time meeting the condition of minimum mass and maintaining the desired rigidity characteristics of the design [13].

The findings of this study may serve as a foundation for future work aimed at optimising the orthoses shape through stiffening and mass reduction. Using the conclusions reached from the modelling, particularly the distribution of principal stress directions and values, it is possible to propose an alignment of stiffening components that work in accordance with the determined principal stress directions. Simultaneously, it is able to lower the mass of the orthoses by decreasing the amount of material in areas of the braces that are not exposed to as much load.

5. Conclusions

The definition of the orthosis working scheme was defined by determining the area of the brace exposed to compressive stress and pursuing its corrective function. We computed the stress distributions inside the orthosis geometry and showed the trajectories of principal stresses to illustrate the "flow of forces" in the basic "three-point pressure system". As a result, areas of the brace that are particularly important in terms of correction were found. The above-mentioned objectives were made achievable by verifying the orthosis form in experimental and numerical simulations. The properly formed computer model serves as the foundation for performing high-reliability numerical simulations with the ultimate goal of optimising orthosis structure. It is clear that the study under consideration is universally applicable and can be easily extended to many other kinds of orthosis.

Author Contributions: Conceptualization, S.G. and P.M.; methodology, S.G. and P.M.; software, S.G.; validation, S.G. and P.M.; formal analysis, S.G. and P.M.; investigation, S.G.; resources, S.G. and P.M.; data curation, S.G. and P.M.; writing—original draft preparation, S.G.; writing—review and editing, P.M.; visualization, S.G.; supervision, P.M.; project administration, S.G. and P.M.; funding acquisition, S.G. and P.M. All authors have read and agreed to the published version of the manuscript.

Funding: The printing of the article was financed from the ZIREG project—Integrated Program of the Bialystok University of Technology for Regional Development, contract no. POWR.03.05.00-00-ZR22/18. Project co-financed by the European Union from the European Social Fund under the Knowledge Education Development Operational Program 2014–2020.

Institutional Review Board Statement: Not applicable.

Informed Consent Statement: Not applicable.

Conflicts of Interest: The authors declare no conflict of interest. The funders had no role in the design of the study; in the collection, analyses, or interpretation of data; in the writing of the manuscript, or in the decision to publish the results.

References

1. Chan, W.Y.; Yip, J.; Yick, K.-L.; Ng, S.-P.; Lu, L.; Cheung, K.M.-C.; Kwan, K.Y.-H.; Cheung, J.P.-Y.; Yeung, K.W.-K.; Tse, C.-Y. Mechanical and Clinical Evaluation of a Shape Memory Alloy and Conventional Struts in a Flexible Scoliotic Brace. *Ann. Biomed. Eng.* **2018**, *46*, 1194–1205. [CrossRef] [PubMed]
2. Raux, S.; Kohler, R.; Garin, C.; Cunin, V.; Abelin-Genevois, K. Tridimensional Trunk Surface Acquisition for Brace Manufacturing in Idiopathic Scoliosis. *Eur. Spine J.* **2014**, *23*, 419–423. [CrossRef] [PubMed]
3. Chan, A.; Lou, E.; Hill, D.; Faulkner, G. Design and Validation of Transducers to Measure Interface Force Distribution in a Spinal Orthosis. *Med. Eng. Phys.* **2012**, *34*, 1310–1316. [CrossRef] [PubMed]
4. Rigo, M.D.; Villagrasa, M.; Gallo, D. A Specific Scoliosis Classification Correlating with Brace Treatment: Description and Reliability. *Scoliosis* **2010**, *12*, 1. [CrossRef]
5. Rigo, M.; Negrini, S.; Weiss, H.; Grivas, T.; Maruyama, T.; Kotwicki, T. TLSO Biomechanics of Correction (Investigating the Rationale for Force Vector Selection). *Scoliosis* **2006**, *5*, 11. [CrossRef]
6. Clin, J.; Aubin, C.-É.; Parent, S.; Labelle, H. Biomechanical Modeling of Brace Treatment of Scoliosis: Effects of Gravitational Loads. *Med. Biol. Eng. Comput.* **2011**, *49*, 743–753. [CrossRef]
7. Clin, J.; Aubin, C.-É.; Parent, S.; Labelle, H. A Biomechanical Study of the Charleston Brace for the Treatment of Scoliosis. *Spine* **2010**, *35*, E940–E947. [CrossRef]
8. Clin, J.; Aubin, C.-E.; Parent, S.; Sangole, A.; Labelle, H. Comparison of the Biomechanical 3D Efficiency of Different Brace Designs for the Treatment of Scoliosis Using a Finite Element Model. *Eur. Spine J.* **2010**, *19*, 1169–1178. [CrossRef]
9. Cobetto, N.; Aubin, C.E.; Parent, S.; Clin, J.; Barchi, S.; Turgeon, I.; Labelle, H. Effectiveness of Braces Designed Using Computer-Aided Design and Manufacturing (CAD/CAM) and Finite Element Simulation Compared to CAD/CAM Only for the Conservative Treatment of Adolescent Idiopathic Scoliosis: A Prospective Randomized Controlled Trial. *Eur. Spine J.* **2016**, *25*, 3056–3064. [CrossRef]
10. Courvoisier, A.; Nesme, M.; Gerbelot, J.; Moreau-Gaudry, A.; Faure, F. Prediction of Brace Effect in Scoliotic Patients: Blinded Evaluation of a Novel Brace Simulator—an Observational Cross-Sectional Study. *Eur. Spine J.* **2019**, *28*, 1277–1285. [CrossRef]
11. Nijssen, J.P.A.; Radaelli, G.; Herder, J.L.; Kim, C.J.; Ring, J.B. Design and Analysis of a Shell Mechanism Based Two-Fold Force Controlled Scoliosis Brace. *Mech. Robot.* **2017**, *5*, 1–12. [CrossRef]
12. Weiss, H.-R.; Kleban, A. Development of CAD/CAM Based Brace Models for the Treatment of Patients with Scoliosis-Classification Based Approach versus Finite Element Modelling. *Asian Spine J.* **2015**, *9*, 661–668. [CrossRef] [PubMed]
13. Liao, Y.-C.; Feng, C.-K.; Tsai, M.-W.; Chen, C.-S.; Cheng, C.-K.; Ou, Y.-C. Shape Modification of the Boston Brace Using a Finite-Element Method with Topology Optimization. *Spine* **2007**, *32*, 3014–3019. [CrossRef] [PubMed]
14. Périé, D.; Aubin, C.E.; Lacroix, M.; Lafon, Y.; Labelle, H. Biomechanical Modelling of Orthotic Treatment of the Scoliotic Spine Including a Detailed Representation of the Brace-Torso Interface. *Med. Biol. Eng. Comput.* **2004**, *42*, 339–344. [CrossRef]
15. Périé, D.; Aubin, C.E.; Petit, Y.; Labelle, H.; Dansereau, J. Personalized Biomechanical Simulations of Orthotic Treatment in Idiopathic Scoliosis. *Clin. Biomech.* **2004**, *19*, 190–195. [CrossRef]
16. Chung, C.L.; Kelly, D.M.; Steele, J.R.; DiAngelo, D.J. A Mechanical Analog Thoracolumbar Spine Model for the Evaluation of Scoliosis Bracing Technology. *J. Rehabil. Assist. Technol. Eng.* **2018**, *5*, 2055668318809661. [CrossRef]
17. Guan, T.; Zhang, Y. Determination of Three-Dimensional Corrective Force in Adolescent Idiopathic Scoliosis and Biomechanical Finite Element Analysis. *Front. Bioeng. Biotechnol.* **2019**, *8*, 963. [CrossRef]
18. Fortin, D.; Cheriet, F.; Beauséjour, M.; Debanné, P.; Joncas, J.; Labelle, H. A 3D Visualization Tool for the Design and Customization of Spinal Braces. *Comput. Med. Imaging Graph.* **2007**, *31*, 614–624. [CrossRef]
19. Rigo, M.; Jelačić, M. Brace Technology Thematic Series: The 3D Rigo Chêneau-Type Brace. *Scoliosis* **2017**, *12*, 10. [CrossRef]
20. Mrozek, P. The Use of Electronic Speckle Pattern Interferometry for Evaluation of Machine Tool Static Stiffness. *Lasers Eng.* **2019**, *43*, 81–99.
21. Macek, W.; Macha, E. The Control System Based on FPGA Technology For Fatigue Test Stand MZGS-100 PL. *Arch. Mech. Eng.* **2015**, *62*, 85–100. [CrossRef]
22. Sanz-Pena, I.; Arachchi, S.; Halwala-Vithanage, D.; Mallikarachchi, S.; Kirumbara-Liyanage, J.; McGregor, A.; Silva, P.; Newell, N. Characterising the Mould Rectification Process for Designing Scoliosis Braces: Towards Automated Digital Design of 3D-Printed Braces. *Appl. Sci.* **2021**, *11*, 4665. [CrossRef]
23. Grycuk, S.; Mrozek, P. Numerical Analysis of Scoliosis Brace. In *The International Conference of the Polish Society of Biomechanics*; Hadamus, A., Piszczatowski, S., Błażkiewicz, M., Syczewska, M., Eds.; Lecture Notes in Networks and Systems; Springer: Cham, Switzerland, 2021; Volume 328, pp. 44–54.
24. Gignac, D.; Aubin, C.; Dansereau, J.; Labelle, H. Optimization Method for 3D Bracing Correction of Scoliosis Using a Finite Element Model. *Eur. Spine J.* **2000**, *9*, 185–190. [CrossRef] [PubMed]
25. Khlif, M.; Masmoudi, N.; Bradai, C. Polypropylene Tensile Test under Dynamic Loading. *J. KONES* **2014**, *21*, 132–138. [CrossRef]
26. Wawruch, P.; Czarnecki, S. Construction of Stress Trajectories in Optimal, Non-Homogeneous Elastic Bodies. In *Advances in Mechanics: Theoretical, Computational and Interdisciplinary Issues*; Kleiber, M., Burczynski, T., Wilde, K., Gorski, J., Eds.; CRC Press: London, UK, 2016; pp. 137–140.
27. Kelly, D.W.; Tosh, M.W. Interpreting Load Paths and Stress Trajectories in Elasticity. *Eng. Comput.* **2000**, *17*, 117–135. [CrossRef]

28. Boston Brace International, Inc. *Reference Manual for the Boston Scoliosis Brace*; Boston Brace International, Inc.: Avon, MA, USA, 2003.
29. Ng, K.J.; Duke, K.; Lou, E. Investigation of Future 3D Printed Brace Design Parameters: Evaluation of Mechanical Properties and Prototype Outcomes. *J. 3D Print. Med.* **2019**, *3*, 171–184. [CrossRef]